Proceedings World Geothermal Congress 2023
Beijing, China, April 17 – 21, 2023

Simulation of wave propagation in a thermoelastic media adopting the L-S theory under the seismic frequency band

Sen Yang, Guochen Wu

School of Geosciences, China University of Petroleum (East China), Qingdao, 266580, China

yangsen_upc@163.com

Keywords: Thermoelastic; Simulation; L-S theory; Forward modeling.

ABSTRACT

Exploration of geothermal resources is important from the energy point of view. As one of the key geophysical exploration methods, classical seismic-wave propagation theory regards the underground medium as completely elastic under isothermal or adiabatic deformation. However, the underground medium is not completely elastic under the influence of temperature. Therefore, studying the propagation process of the thermoelastic wave is of great significance to geothermal exploration. The problem of wave propagation in thermoelastic media can be described based on the L-S theory, considering the effect of temperature on wave propagation. This is important for adopting seismic exploration methods to find geothermal fields. Based on previous research, we realize the numerical simulation of wave propagation in thermoelastic media by adopting staggered-grid and PML absorption boundary and propose an absorption method for the reflection on temperature boundary. Then, the propagation process of thermoelastic waves under the condition of constant temperature and the variable temperature was compared. It is observed that with the increase of reference temperature, the amplitude of the E-wave becomes larger, and the wave velocity becomes faster. The new wavefield simulation method can effectively synthesize seismic records for following inversion work. This method lays a foundation for thermoelastic wave imaging and inversion.

1. INTRODUCTION

The wave propagation in the underground medium is affected by temperature. However, the classical seismic wave propagation theory does not consider the temperature effect. It regards the underground medium as completely elastic, which cannot accurately simulate the propagation process in the high-temperature medium. As an extension of elastic theory, the thermoelastic theory describes the relationship between elastic deformation and temperature (Li et al., 2021; Hou et al., 2021). Based on the theory of thermoelasticity, studying wave propagation in the high-temperature medium is of great significance to exploring geothermal resources.

In 1956, Biot proposed the coupled thermoelasticity (CTE) theory, deduced the heat conduction/thermoelastic coupled equation based on the Fourier law of heat conduction. However, the solution of the heat conduction equation derived from CTE theory contradicts the special relativity, contrary to the fact that waves propagate within a finite range of velocities. Lord and Shulman (1967) studied the L-S theory (generalized thermoelasticity theory, GTE). According to the L-S theory, the thermal relaxation time was introduced to correct Fourier's law of heat conduction to ensure that the heat propagation velocity is within a limited range to overcome the paradox of infinite heat wave velocity. Green and Lindsay (1972) further proposed the G-L theory and modified the motion equation and heat conduction equation by introducing two thermal relaxation times.

Numerical simulation of the wave equation is an important method to study the propagation characteristics of the seismic wave field, such as the finite difference method (Madariaga, 1976; Virieux, 1984; Veres et al., 2013), finite element method (Marfurt, 1984; Serón et al., 1990), boundary element method (Kawase, 1988; Fu and Mou, 1994). The finite difference method is widely used in seismic wave numerical simulation due to its high computing speed and easy realization. In terms of numerical simulation of thermoelastic waves, Carcione et al (2019a) decomposed the stiff equation into stiff and non-stiff parts according to the GTE theory. They studied the simulation method of the thermoelastic wave equation (Carcione et al., 2019a, 2019b). Wang et al (2020) studied Green's function of the thermoelastic equation based on the generalized thermoelasticity theory. Li et al (2021) studied the first order velocity stress temperature differential equation, and realized the wave field simulation based on the rotated staggered grid pseudo-spectral method. Hou et al (2021) adopted the rotated staggered grid and CPML absorption boundary to improve the wave field simulation. Yang et al (2022) further considered the absorption boundary of T-wave propagation and studied the 2D numerical simulation method of the first-order thermoelastic wave equation with a staggered grid.

In this paper, we first derive the thermoelastic wave discrete format based on the L-S theory according to the work of Carcione et al (2019) and Li et al (2021). Then, we derive the PML absorbing boundary schem, and the numerical simulation of the thermoelastic wave field is realized using staggered grids. Finally, the method is validated by a layered heterogeneous model, and the computing speed is optimized to ensure accuracy and stability.

2. 3D FIRST-ORDER VELOCITY-STRESS-TEMPERATURE DIFFERENTIAL EQUATION

The classical thermoelastic theory is based on the equation of motion and Fourier heat conduction equation. Because of the parabolic nature of the classical heat conduction equation, thermal disturbances propagate at infinite speed in this expression. Although this prediction applies to many engineering problems, it expressed a property that contradicts special relativity, contrary to the fact that waves travel at finite velocities.

2.1 Thermoelastic wave equation based on the L-S theory

Lord and Shulman (1967) introduced a time relaxation factor based on the first and second laws of thermodynamics to overcome the paradox of infinite heat wave velocity. On this basis, Carcione et al. (2019) deduced the new displacement-temperature coupled wave equations. And combined with the stress-strain, stress-displacement, and strain-displacement equations, we can derive the first-order velocity-stress-temperature differential equations.

$$
\begin{aligned}
&\dot{v}_i = \eta_i = (1/\rho)\left(\sigma_{ij,j} - f_i\right)\\
&\dot{\sigma}_{ij} = \mu\left(v_{i,j} + v_{j,i}\right) + \lambda v_{i,i}\delta_{ij} - \beta\xi\delta_{ij} + \dot{f}_{ij}\\
&\dot{T} = \xi\\
&\dot{\xi} = (1/c\tau)\left[k\Delta T_{,ii} - T_0\beta\left(v_{i,i} + \tau\eta_{i,i}\right) - q\right] - (1/\tau)\xi
\end{aligned}
\tag{1}
$$

Where v and σ denotes the components of the velocity and stress tensor, " ,i " denotes a spatial derivative, ρ is density, the dot above a variable indicate the first-order time derivative, and f_i denotes the external body force component, λ and μ are Lamé constants, β is the thermal modulus, which can be expressed as $\beta=(3\lambda+2\mu)\alpha$, α denotes the linear thermal expansion coefficient, k is the thermal conductivity, Δ is the Laplacian operator, c is the specific heat of the unit volume in the absence of deformation, ΔT is the temperature increment relative to the reference temperature T_0. τ is the thermal relaxation time, which can be obtained with $\tau=k/(c\cdot v_p^2)$ (Rudgers, 1990). q is the heat source.

2.2 Numerical solutions to wave propagation equations

2.2.1 A staggered grid difference scheme considering PML boundary

The staggered grid is the most common method to obtain numerical solutions for wave propagation, which has the advantages of easy implementation, small memory consumption, and fast calculation speed. At the same time, we consider the boundary reflection problem in the numerical simulation process. We derive the staggered grid difference scheme of the three-dimensional first-order velocity-stress-temperature equation with the PML absorbing boundary.

$$
\begin{aligned}
&v_{i,\,j}(t+\Delta t/2) = \left(1/\left(2+dx_j\cdot\Delta t\right)\right)\left[\left(2\text{-}dx_j\cdot\Delta t\right)\cdot v_{i,j}(t-\Delta t/2) + 2\Delta t\cdot\sigma_{ij,j}\right]\\
&\sigma_{ij,\,j}(t) = \left(1/\left(2+dx_j\cdot\Delta t\right)\right)\left\{\left(2\text{-}dx_j\cdot\Delta t\right)\cdot\sigma_{ii,j}(t-\Delta t) + 2\Delta t\left[\mu\left(v_{i,j}+v_{j,i}\right) + \lambda v_{i,i}\delta_{ij}\right]\right\}\\
&\sigma_{ii,\,\xi}(t) = \tau\beta\left[\exp(-\Delta t/\tau) - 1\right]\xi(t-\Delta t)\\
&T(t) = T(t-\Delta t) + \Delta t\cdot\xi(t)\\
&\xi_{T,\,i}(t) = \left(1/\left(1+dx_i\cdot\Delta t\right)\right)\left[\left(1\text{-}dx_i\cdot\Delta t\right)\cdot\xi_{T,\,i}(t-\Delta t) - \left(dx_i\right)^2\int\xi_{T,\,i}\,dt + 2\Delta t\cdot(k/c\tau)\cdot T_{,\,ii}\right]\\
&\xi_{v_{i,\,i}}(t) = \left(1/\left(2+dx_i\cdot\Delta t\right)\right)\left[\left(2\text{-}dx_i\cdot\Delta t\right)\cdot\xi_{v_{i,\,i}}(t-\Delta t) - 2\Delta t\cdot\left(T_0\beta/c\tau\right)\cdot v_{i,\,i}\right]\\
&\xi_{\eta_{i,\,i}}(t) = \left(1/\left(2+dx_i\cdot\Delta t\right)\right)\left[\left(2\text{-}dx_i\cdot\Delta t\right)\cdot\xi_{\eta_{i,\,i}}(t-\Delta t) - 2\Delta t\cdot\left(T_0\beta/c\tau\right)\cdot\eta_{i,\,i}\right]\\
&\xi_{\xi}(t) = \left[\exp(-\Delta t/\tau) - 1\right]\xi(t-\Delta t)
\end{aligned}
\tag{2}
$$

Where dx and Δt denotes the space grid interval and time step. The specific grid node distribution is shown in Figure 1.

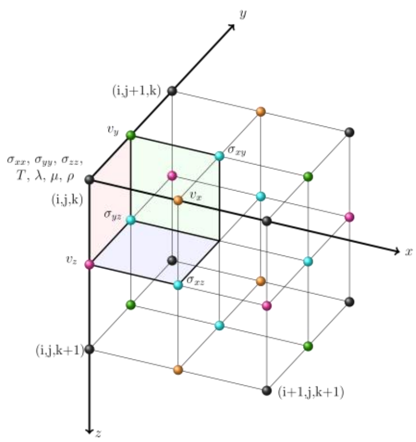

Figure 1: Staggered-grid for the discretization of the thermoelastic equations and partial difference coefficients.

2.2.2 Numerical dispersion and stability

Numerical dispersion significantly affects the accuracy of finite difference wavefield simulation. Moreover, similar to the numerical dispersion in space, the discretization in time must also meet the Courant-Friedrichs-Levy (CFL) stability criterion. Therefore, we can use the numerical dispersion and stability conditions of the three-dimensional elastic wave equation to solve the numerical simulation of thermoelastic waves.

$$dx = dh \le \frac{\lambda_{\min}}{n} = \frac{v_{\min}}{n f_{\max}} \quad \Delta t \le \frac{dh}{h\sqrt{3} v_{\max}} \tag{3}$$

Where, the factor h depends on the order of the difference operator, v_{max} and v_{min} are the maximum and minimum velocities of the given model, λ_{min} denotes the minimum wavelength, and f_{max} represents the maximum frequency of the source signal.

3. NUMERICAL EXAMPLES AND ANALYSIS

The method was verified with a double-layer coupling model of an elastic media, thermoelastic media (with constant and variable temperature) with a 121×121×121 grid having a cell size of 5m×5m×5m. The time step is 0.5ms, and a vertical elastic source with a domain frequency 20Hz is located on the middle top of the given model. Moreover, the elastic constants are as follows: v_{p0}=1500 m/s, v_{p1}=3000 m/s, v_{s0}=898 m/s, v_{s1}=1796 m/s, k=105 m·kg·s^{-3}·K^{-1}, ρ=3650 kg·m^{-3}, c=117 kg·m^{-1}·s^{-3}·K^{-1}, T_0=300 K.

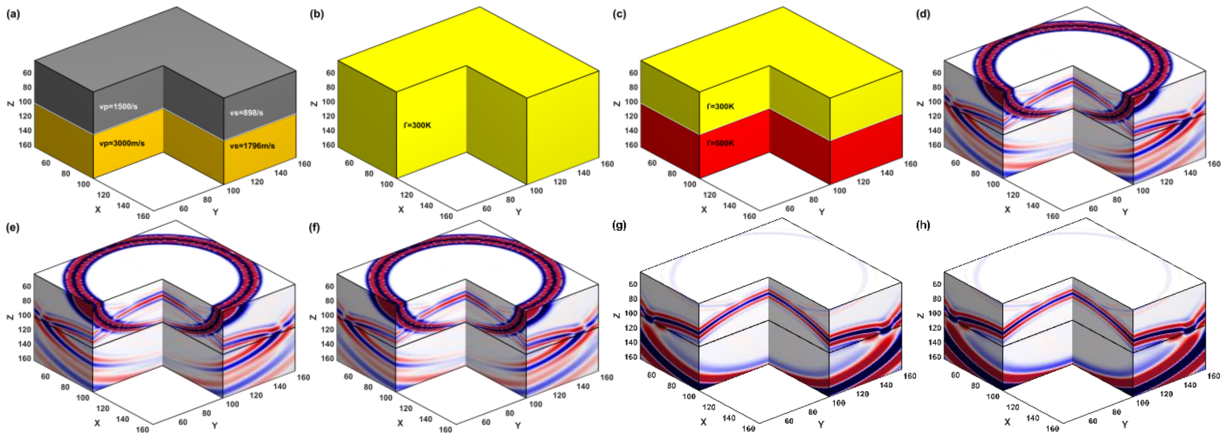

Figure 2: Wavefield snapshots (t=370 ms) of the double-layered model when using a vertical elastic source (f_m=20 Hz). (a) Elastic model; (b) Thermoelastic model (with constant temperature); (c) Thermoelastic model (with variable temperature); (d) V_z of the elastic wavefield; (e) V_z of the thermoelastic wavefield (with constant temperature); (f) V_z of the thermoelastic wavefield (with variable temperature); (g) ΔT of the thermoelastic wavefield (with constant temperature); (h) ΔT of the thermoelastic wavefield (with variable temperature);

Figure 2 shows the wavefield snapshots (t=370 ms) of the double-layered model when using a vertical elastic source (f_m=20 Hz). We adopted an elastic source loaded on the vertical component of the velocity to verify the effect of PML boundary treatment (PML=40). It can be seen that the boundary difference scheme derived in this paper can well suppress the boundary reflection. We also considered boundary reflection suppression to the temperature increment field, which proved the good effect of this method.

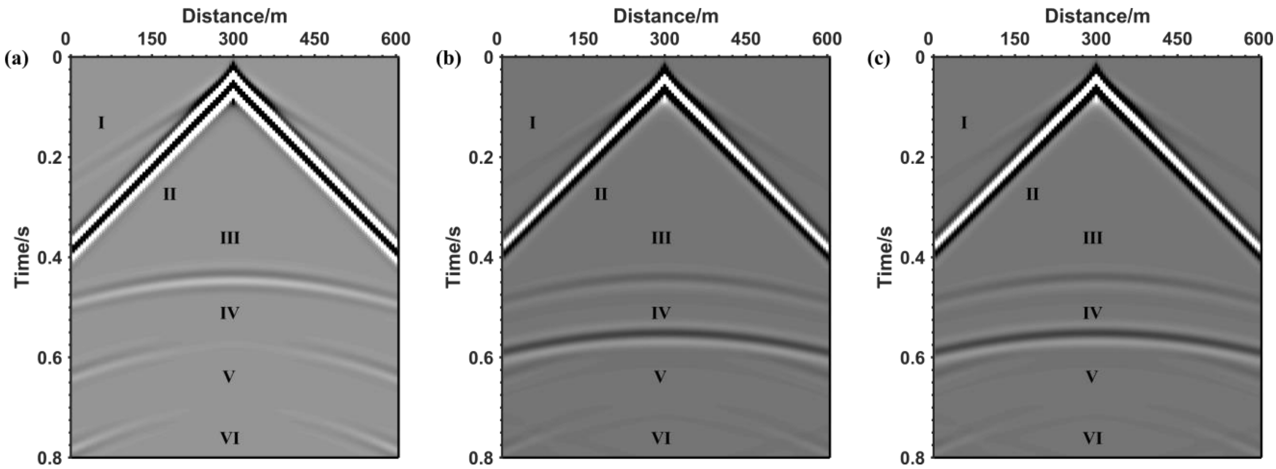

Figure 3: V_z of the synthetic seismogram when using a vertical elastic source (f_m=20 Hz). (a) Elastic double-layered model; (b) Thermoelastic double-layered model, constant temperature; (c) Thermoelastic double-layered model, variable temperature.

The seismogram of the vertical component of particle velocity and the events of various waves are shown in Fig. 3. Where, I is the direct P wave (In Fig. 3b and 3c, it is the E wave after the coupling of the P wave and temperature), II is the direct S wave, and III represents the P-P wave (In Fig. 3b and 3c, it is the E-P wave) reflected at the layered interface. IV represents the P-S wave (In Fig. 3b and 3c, it is the E-S wave) reflected at the layered interface, V represents the S-P wave reflected at the layered interface, VI represents the S-S wave reflected at the layered interface. Moreover, as we can see from the seismograms in Fig. 3a and 3b, the direct and reflected waves appear earlier and faster in the thermoelastic (constant temperature) than in the elastic model. Furthermore, the seismic records of direct and reflected waves in the thermoelastic (variable temperature, Fig. 3c) appear earlier than those in the thermoelastic (constant temperature). With the increase of the reference temperature, the amplitude of the E wave becomes larger, and the wave velocity becomes faster.

4. CONCLUSIONS

We used the staggered grid method to obtain the numerical solution of the thermoelastic wave equation based on the L-S theory and extended this work to the three-dimensional data space. After considering the numerical dispersion and stability conditions, this numerical simulation method can operate stably under the seismic frequency band (2-120Hz). In addition, considering the boundary reflection problem in the simulation process, we also derived a three-dimensional boundary form for PML absorption of thermoelastic waves. The proposed expression of the PML absorption boundary went well on the velocity and stress components and introduced to the temperature increment, which achieved a good absorption effect. The new wave field simulation method can effectively synthesize seismic records for following inversion work and is significant to geothermal exploration.

ACKNOWLEDGEMENTS

We would like to acknowledge the sponsorship of National Natural Science Foundation of China (42030103).

REFERENCES <HEADING 1 STYLE>

Biot, M. A.: Thermoelasticity and irreversible thermodynamics, Journal of applied physics, 1956, 27(3): 240-253.

Carcione, J. M., Cavallini, F., Wang, E., et al.: Physics and simulation of wave propagation in linear thermoporoelastic media, Journal of Geophysical Research: Solid Earth, 2019a, 124(8): 8147-8166.

Carcione, J. M., Wang, Z. W., Ling, W., et al.: Simulation of wave propagation in linear thermoelastic media, Geophysics, 2019b, 84(1): T1-T11.

Fu, L. Y., and Mou, Y. G.: Boundary element method for elastic wave forward modeling, Chin J Geophys, 1994, 37(4): 521-529.

Green, A. E., and Lindsay, K. A.: Thermoelasticity, Journal of elasticity, 1972, 2(1): 1-7.

Hou, W., Fu, L. Y., Carcione, J. M., et al.: Simulation of thermoelastic waves based on the Lord-Shulman theory, Geophysics, 2021, 86(3): T155-T164.

Kawase, H.: Time-domain response of a semi-circular canyon for incident SV, P, and Rayleigh waves calculated by the discrete wavenumber boundary element method, Bulletin of the seismological Society of America, 1988, 78(4): 1415-1437.

Lord, H. W., and Shulman, Y.: A generalized dynamical theory of thermoelasticity, Journal of the Mechanics and Physics of Solids, 1967, 15(5): 299-309.

Li, Y., Liu, C., Guo, Z., et al.: Simulation and characteristics analysis of a wavefield in a thermoelastic medium adopting the rotated staggered-grid pseudo-spectral method and LS theory, Science China Earth Sciences, 2021, 64(8): 1390-1408.

Madariaga, R.: Dynamics of an expanding circular fault, Bulletin of the Seismological Society of America, 1976, 66(3): 639-666.

Marfurt, K. J.: Accuracy of finite-difference and finite-element modeling of the scalar and elastic wave equations, Geophysics, 1984, 49(5): 533-549.

Serón, F. J., Sanz, F. J., Kindelan, M., et al.: Finite-element method for elastic wave propagation, Communications in applied numerical methods, 1990, 6(5): 359-368.

Virieux, J.: SH-wave propagation in heterogeneous media: Velocity-stress finite-difference method, Geophysics, 1984, 49(11): 1933-1942.

Veres, I. A., Berer, T. and Burgholzer, P.: Numerical modeling of thermoelastic generation of ultrasound by laser irradiation in the coupled thermoelasticity, Ultrasonics, 2013, 53(1): 141-149.

Wang, K., Peng, S., Lu, Y., et al.: The velocity-stress finite-difference method with a rotated staggered grid applied to seismic wave propagation in a fractured medium, Geophysics, 2020, 85(2): T89-T100.

Yang, S., Wu, G., Shan, J., et al.: Simulation of Wave Propagation in a Thermoelastic Media Adopting the Staggered-Grid and LS Theory, European Association of Geoscientists & Engineers, 83rd EAGE Annual Conference & Exhibition, Madrid, Spain 2022(1): 1-5.